"Physics of Auroral Phenomena", Proc. XLVII Annual Seminar, Apatity, pp. 20-23, 2024

Polar Geophysical Institute

DOI: 10.51981/2588-0039.2024.47.004

VERY INTENSE SUBSTORMS IN THE MAGNETIC STORMS OF FEBRUARY AND MARCH 2023

N.G. Kleimenova[1], L.I. Gromova[2], I.V. Despirak[3], S.V. Gromov[2], L.M. Malysheva[1], A.A. Lubchich[3]

[1]*Schmidt Institute Physics of the Earth RAS, Moscow, Russia;* e-mail: *ngk1935@yandex*
[2]*Pushkov Institute of Terrestrial Magnetism, Ionosphere, and Radio Wave Propagation, Moscow, Troitsk, Russia*
[3]*Polar Geophysical Institute, Apatity, Russia*

Abstract. Here we analyzed four very intense substorms with the *AL*-index reached ~ -1500 nT and recorded in the main phases of the strong magnetic storms on 27 February and on 23-24 March 2023. The global dynamics of the considered very intense substorms have been studied basing on the AMPERE satellite data provided the maps of the ionospheric and field aligned currents (*FAC*) distributions in the planetary scale. These maps are constructed by analyzing the magnetometer measurements from the Iridium constellation of 66 simultaneous low-altitude (780 km) communication satellites. The common features of the considered intense substorms have been established. It was found that in the substorm intensity maximum, there was the strong morning-side magnetic vortex with clockwise rotation, indicating an intensification of the downward *FAC*s, probably associated with the enhanced magnetosphere-ionosphere convection. The strongest westward electrojet was observed in the early morning sector and it was accompanied by the significant increasing of the post-noon eastward electrojet as it was found by [*Despirak et al.*, 2021, 2022] to be typical for the supersubstorms. The large-scale eastward electrojet with intensity comparable to the westward electrojet, occurred at lower latitudes in huge longitudinal area - from the afternoon to the late evening. The latitude area between westward and eastward electrojets can be referred to the conventional Harang region.

Introduction

The very strong substorms with intensity, estimated by *SML*-index (this index is described in [*Newell and Gjerloev*, 2011]), as *SML* values < -2500 nT, have been classified as supersubstorms (*SSS)* [*Tsurutani et al.*, 2015] basing on the analysis of the *SML*-index in the Solar Cycly 23 (1996 to 2009), that is in the era of increased solar activity. However. still now this selecting criterion does not have clear physical justifications. Later on in some papers, the *SML* values defining a *SSS* events were not so strong. For instance, *Despirak et al.* [2019] attributed the substorms to the *SSS*-type with *SML* < -2000 nT. In another paper, *Zong et al.* [2021] focusing on interplanetary shocks response, used the *AE*-index *(AE = AL+AU*) values as the criterion of the *SSS* definition and termed the intense substorms with 1000 < *AE* < 2000 nT the "strong substorms", and substorms with *AE* > 2000 nT called the "supersubstoms". Thus, the quantitative criteria defining a *SSS* propose by Tsurutani and Zong are very different, and there were no clear morphological and physical definition of *SSS*.

According to statistical study by *Zong et al.* [2021], the "strong substorms" and supersubstorms could be triggered by sudden changes of solar wind dynamic pressure, most likely under the southward interplanetary magnetic field (IMF). They found that the most intense substorm didn't occur during the main phase of a storm but during the initial phase of the strong magnetic storm, which corresponding to the sheath region just behind the interplanetary shock. *SSSs* are usually observed during interplanetary magnetic cloud or Sheath passage [*Hajra et al.*, 2016; *Despirak et al.*, 2019].

Probably, with coming the era of decreased solar activity, the intensity of magnetic storms and substorns as well as the number of *SSS* events significantly reduced. Really, in the Solar Cycle 24, only several *SSS* events have been recorded.

The aim of this paper was an analysis of spatio-temporal features of several storm-associated intense substorms with *AL* index values in order of 1500 nT, recorded during the main phases of the strong magnetic storms on 26-27 February 2023 and on 23-24 March 2023.

Observations and Discussion

Our analysis of the global dynamics of these very intense substorms has been studied basing on of the AMPERE project (https://ampere.jhuapl.edu) data provided the planetary maps of the ionospheric and field aligned currents (FAC) distributions, at 10 min averages with the 2 min cadence [e.g., *Anderson et al.*, 2014]. The maps are constructed by using magnetometer observations from the Iridium constellation of 66 low-altitude (780 km) globally distributed communication satellites.

Here we analyzed the intense substorms during the strong magnetic storms in February and March 2023. Figure 1 demonstrates the variations of *AL*-index values during these storms and shows the generation, at least, of four intense substorms with the *AL*-index ~ -1500 nT or little higher. These data are taken from World Data Center for Geomagnetism, Kyoto (http://wdc.kugi.kyoto-u.ac.jp). Unfortunately, in the present time, the World Data Center has not yet provided users with digital index data, and the presented in Figure 1 graphics of row *AL*-index data can include impulsive noise and spiks.

(a)

(b)

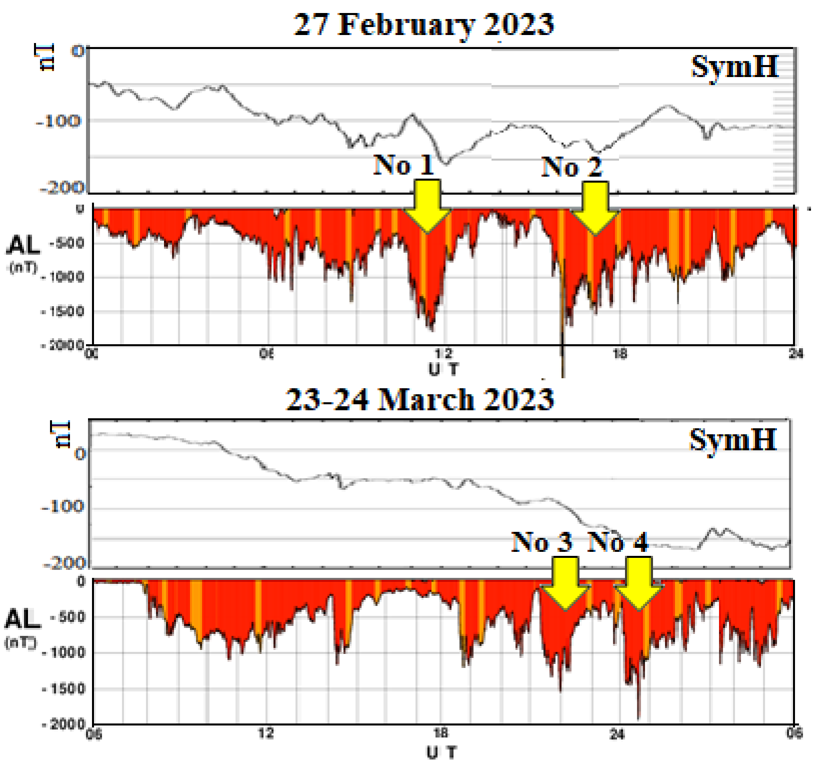

Figure 1. The variations of *AL*-index values during the main phases of the strong magnetic storms (a) - on 27 February 2023 (*SymH* ~ -150 nT), (b) – on 24 March 2023 (*SymH* ~ -170 nT). The very intense substorms are shown by yellow arrows.

The substorm intensity of the substorms No 1 and No 2 was higher than the intensity of the substorms No 3 and No 4 despite the ring current *(Dst*-values) was stronger in the second storm. The maximal values of *AL*-index during the substorms No 3 and No 4 (March magnetic storm) were almost similar, however, the substorm No 3 has been developed under *Dst* ~ -70 nT, and the substorm No 4 – under *Dst* ~ -140 nT. Thus, there was no linear relationship between the substorm intensity and the symmetric ring current intensification (*SymH/Dst* values).

The global distributions of the ionospheric electrojets (green color) and FACs (blue and red color correspondently to the downward and upward FACs) are shown as the AMPERE maps in the time interval correspondent to the maxima of the expansion phases of the considered intense substorms No 1-4. The maps are presented in Figure 2 (27 February 2023 magnetic storm) and Figure 3 (23-24 March 2023 magnetic storm).

We compared the global distributions of the ionospheric electrojets and FACs in the maximum of the expansion phase of the studied intense substorms (Figure 2 and Figure 3) with the same feature of another intense storm-time substorm recorded on 17 March 2015 (see Figure 4). We found that all maps in Figures 2-4 are looking very similar. Each considered event demonstrates the presence of the large morning vortex with the clockwise rotation indicating an enhancement of the morning downward Field Aligned Currents (FACs) marked by blue on the AMPERE maps.

At the westward edge of the vortex, the westward electrojet shifts poleward to the evening side. Simultaneously the strong large-scale eastward electrojet with intensity comparable to the westward electrojet, occurs at lower latitudes in huge longitudinal area - from the afternoon to the late evening. The large latitude area between them can be referred to the conventional Harang discontinuity. The strongest eastward electrojet values are observed in dusk (~17-20 MLT). It is interesting to note that the strong enhancement of the eastward electrojet was typical for supersubstorms [e.g., *Fu et al.*, 2021; *Zong et al.*, 2021; *Despirak et al.*, 2021; 2022] and can be a result of the formation of an additional current wedge structure around dusk [*Fu et al.*, 2021], suggesting a linkage between intense substorms and the ring current. The ionospheric eastward dusk current located at the inner magnetosphere is closed by the partial ring current.

The morning magnetic vortex can be explained by the model of the double current wedge formation [*Gjerloev and Hoffman*, 2014] presented in Figure 5, included a poleward shift of the westward electrojet connecting the post-midnight and pre-midnight components.

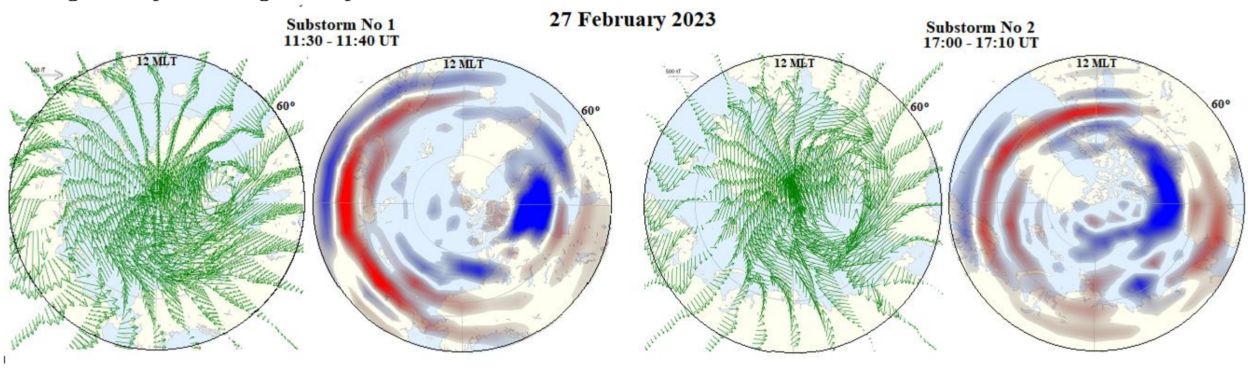

Figure 2. The ionospheric electrojets (shown by green) and the FAC distribution (the downward FACs are shown by blue, the upward FACs are shown by red) after the AMPERE data in maximum of the expansion phases of two intense substorms (No1 and No 2) on 27 February 2023.

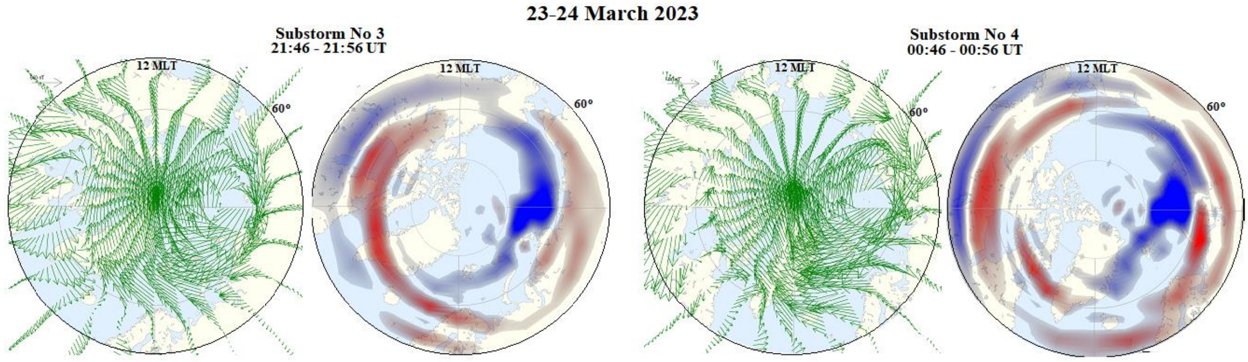

Figure 3. The ionospheric electrojets (green) and the FAC distribution after the AMPERE data in maximum of intensity substorms No 3 and No 4 on 24 March 2023.

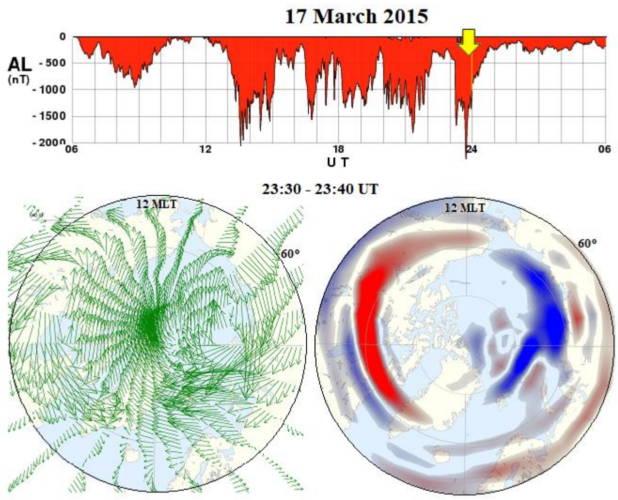

Figure 4. The ionospheric electrojets (green) and the FAC distribution after the AMPERE data in the maximum intensity of another strong storm-time substorm on 17 March 2015.

At ionospheric altitudes, the key difference between the two wedge configurations (see Fig. 5) lies in the midnight region. *Gjerloev and Hoffman* [2002] found a distinct region of very low fields in the pre-midnight region referred to the conventional Harang discontinuity, which separates poleward fields at lower latitudes and equatorward fields at higher latitudes. This Harang region effectively suppressed convection [*Gjerloev and Hoffman*, 2002] and pre-midnight westward electrojet. The two-wedge current system [*Gjerloev and Hoffman*, 2014] for the westward electrojet links the ionosphere to the magnetosphere: a bulge current wedge located in the pre-midnight region just equatorward of the open-closed field line boundary and another three-dimensional current wedge system located in the post-midnight region well within the auroral oval.

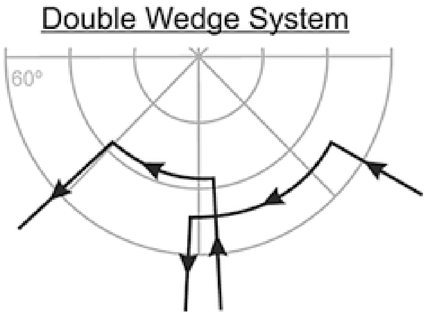

Figure 5. The schematic-configurations of two current wedge systems shifted in local time and latitude, only the net field-aligned currents and the ionospheric Hall currents are shown [after *Gjerloev and Hoffman*, 2014].

Summary

Here we analyzed four very intense substorms with the *AL*-index reached about -1500 nT and recorded in the main phases of the strong magnetic storms on 27 February and on 23-24 March 2023. The global dynamics of the considered intense substorms have been studied basing on the AMPERE satellite data provided the maps of the ionospheric and field aligned currents (FAC) distributions in the planetary scale. It was found that the common features of the considered intense substorms were very similar each other.

It has been established that in the substorm intensity maximum, there was developed the strong morning-side magnetic vortex with clockwise rotation, indicating an intensification of the downward FAC, probably associated with the enhanced magnetosphere-ionosphere convection.

The large-scale eastward electrojet with intensity comparable to the westward electrojet, occurs at lower latitudes in huge longitudinal area - from the afternoon to the late evening. The latitude area between westward and eastward electrojets can be referred to the conventional Harang region.

References

Anderson B.J., Korth H., Waters C.L., Green D.L., et al. Development of large-scale Birkeland currents determined from the Active Magnetosphere and Planetary Electrodynamics Response Experiment. Geophys. Res. Lett. V. 41, No. 9, P. 3017–3015, 2014. https://doi.org/10.1002/2014GL059941

Despirak I.V., Lyubchich A.A., Kleimenova N.G. Supersubstorms and conditions in the solar wind. Geomagnetism and Aeronomy. V. 59, P. 170–176, 2019. https://doi.org/10.1134/S0016793219020075

Despirak I.V., Lyubchich A.A., Kleimenova N.G., Gromova L.I., Gromov S.V., Malysheva L.M. Longitude geomagnetic effects of the supersubstorms during the magnetic storm of March 9, 2012. Bulletin of the Russian Academy of Sciences: Physics. V.85, No. 3, P. 246–251, 2021. doi: 10.3103/S1062873821030096

Despirak I.V., Kleimenova N.G., Lyubchich A.A., Setsko P.V., Gromova L.I., Werner R. Global development of the supersubstorm of May 28, 2011. Geomagnetism and Aeronomy. V. 62, No. 3, P. 199–208, 2022. https://doi.org/10.1134/S0016793222030069

Fu H., Yue C., Zong Q.-G., Zhou X.-Z., Fu S. Statistical characteristics of substorms with different intensity. J. Geophys. Res.: Space Physics. V. 126, e2021JA029318, 2021. https://doi.org/10.1029/2021JA029318

Gjerloev J.W., Hoffman R.A. Currents in auroral substorms. J. Geophys. Res. V. 107(A8), 2002. doi:10.1029/2001JA000194

Gjerloev J.W., Hoffman R.A. The large-scale current system during auroral substorms. J. Geophys. Res.: Space Physics. V. 119, P. 4591–4606, 2014. https://doi.org/10.1002/2013JA019176

Hajra R., Tsurutani B.T., Echer E., Gonzalez W.D., Gjerloev J.W. Supersubstorms (SML < -2500 nT): Magnetic storm and solar cycle dependences. J. Geophys. Res. V. 121, No. 8, P. 7805–7816, 2016. doi:10.1002/2015JA021835

Newell P.T., Gjerloev J.W. Evaluation of SuperMAG auroral electrojet indices as indicators of substorms and auroral power. J. Geophys. Res. V. 116, A12211, 2011. doi: 10.1029/2011JA016779

Tsurutani B.T., Hajra R., Echer E., Gjerloev J.W. Extremely intense (SML ≤ -2500 nT) substorms: isolated events that are externally triggered? Ann. Geophys. V. 33, P. 519–524, 2015. https://doi.org/10.5194/angeocom-33-519-2015

Zong Q.-G., Yue C., Fu S.-Y. Shock induced strong substorms and super substorms: Preconditions and associated oxygen ion dynamics. Space Science Review. V. 217:33, 2021. https://doi.org/10.1007/s11214-021-00806-x